Acta Crystallographica Section B
Structural Science
ISSN 0108-7681

Direct observation of various reaction pathways of arylnitrenes in different crystal environments caused by acid–base complex formation

Takahiro Mitsumori, Akiko Sekine,* Hidehiro Uekusa and Yuji Ohashi

Department of Chemistry and Materials Science, Tokyo Institute of Technology, O-okayama, Meguro-ku, Tokyo 152-8551, Japan

Correspondence e-mail: asekine@chem.titech.ac.jp

Received 17 March 2010
Accepted 13 September 2010

The structures of reaction intermediates, arylnitrenes and their final products have been successfully analyzed by X-rays using acid–base complex formation. The acid–base complexes of 2-azidobenzoic acid (2*a*), 3-azidobenzoic acid (3*a*) and 4-azidobenzoic acid (4*a*) were made with dibenzylamine (db), *N*-benzyl-2-phenylethylamine (bp) and dicyclohexylamine (dc). For the complex crystals of (3*a*) and db (3*a*-db), and (4*a*) and db (4*a*-db) two forms of (I) and (II) were obtained. Eight types of complex crystals, (2*a*-db), (3*a*-db-I), (3*a*-db-II), (3*a*-dc), (4*a*-db-I), (4*a*-db-II), (4*a*-bp) and (4*a*-dc), suitable for X-ray analysis were obtained. When the crystals were irradiated with UV light at low temperatures, the reactions proceeded keeping the single-crystal form in the five crystals (2*a*-db), (3*a*-db-I), (3*a*-db-II), (3*a*-dc) and (4*a*-bp). Less than 25% of each azidobenzoic acids was transformed into an arylnitrene and dinitrogen. In three crystals the arylnitrenes produced gave new final products; 2,1-benzisoxazolone was observed for (2*a*-db) and *trans*-azobenzenes (*i.e.* dimerized nitrenes) were obtained for (3*a*-db-II) and (4*a*-bp). For (3*a*-db-I) and (3*a*-dc) the intermediate arylnitrenes were observed but did not transform to new products. All the structural changes were directly observed by X-ray analysis because the incomplete reactions occurred with retention crystallinity. The crystal environment, including the hydrogen bonding between the benzoic acid and the amine, places restrictions on the movement of the arylnitrene and influences the reaction pathway followed for conversion of the arylnitrene to its final product.

1. Introduction

Since the existence of the reaction intermediate phenylnitrene was proposed by Bertho (1924), a variety of attempts have been made by organic and physical chemists to analyze reaction pathways involving arylnitrene (Scriven, 1984; Platz, 1995; Borden *et al.*, 2000; Karney & Borden, 2001; Gritsan & Plats, 2001). Scheme (I) shows the proposed reaction pathways. The singlet arylnitrene is produced upon photolysis or thermolysis of arylazide (Marcinek *et al.*, 1993; Gritsan *et al.*, 1997; Born *et al.*, 1997). The benzene ring of the singlet arylnitrene expands to an unstable seven-membered ring, azacycloheptatetraene (Chapman & Roux, 1978), and further reaction forms the 3*H*-azepine in amine solvents (Doering & Odum, 1966) or polymerizes with itself to give tar (Horner *et al.*, 1963). In the gas phase singlet arylnitrene gives cyanocyclopentadiene (Crow & Wentrup, 1967). Since the lifetime of the singlet arylnitrene is very short (Gritsan *et al.*, 1999), few intermolecular reactions have been reported. The singlet arylnitrene converts to the triplet state *via* intersystem crossing (ISC). The triplet aryl-

nitrene is more stable energetically than the singlet and has strong biradical properties. It has been reported that the triplet arylnitrenes dimerize to azobenzene (Bertho, 1924) or abstract H atoms to afford primary amines or anilines as the final products (Hall *et al.*, 1968). Such different reaction pathways may be affected by many factors, for example, temperature (Leyva & Platz, 1985), solvents and/or matrices (Dunkin *et al.*, 1997), substituents (Leyva *et al.*, 1986; Li *et al.*, 1988).

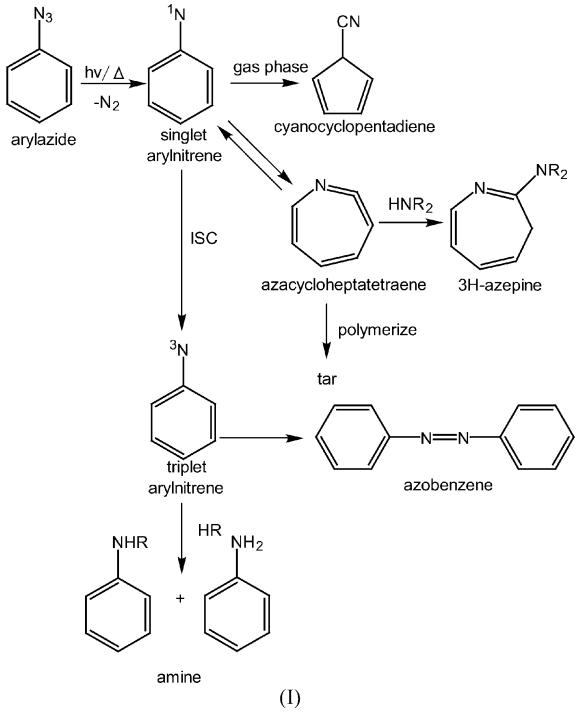

(I)

Although the characteristic behaviors of arylnitrenes in the solid state were studied extensively by Sugawara's group (Mahé *et al.*, 1992; Sasaki *et al.*, 1996, 1998), the presence of arylnitrene could not be determined by X-rays at that time because the quantity was too small. The existence of the arylnitrene was shown by ESR spectroscopy.

Direct observation of the reaction process in a crystal was first carried out using X-ray structure analysis (Ohashi & Sasada, 1977; Ohashi *et al.*, 1981). Such a reaction was called a crystalline-state reaction, since the crystallinity was retained during the whole reaction. A variety of crystalline-state reactions were reviewed (Ohashi, 1988, 1998). Although the reactant and product molecules were clearly shown as disordered structures in a variety of crystalline-state reactions, there are only a few examples of unstable chemical species or reaction intermediates, such as metastable nitrosyl complexes (Rudlinger *et al.*, 1992; Pressprich *et al.*, 1994; Fomitchev & Coppens, 1996; Fomitchev *et al.*, 1998; Kawano, Ishikawa *et al.*, 2000), photo-colored structures (Harada *et al.*, 1999; Naumov *et al.*, 2002; Johmoto *et al.*, 2009), unstable radical intermediates (Kawano *et al.*, 1999; Kawano, Sano *et al.*, 2000) and carbene structures (Kawano *et al.*, 2001; Kawano *et al.*, 2007).

It has been shown that the same technique is applicable to the analysis of unstable arylnitrene structures, and their reaction pathways to the final products have been observed. In a previous paper we reported the structures of 1-azido-2-nitrobenzene before and after photo-irradiation (Takayama *et al.*, 2003). Since benzofuroxan and dinitrogen molecules were observed in the structure after photo-irradiation, it was confirmed that the reaction proceeded as shown in Scheme (II*a*). However, it was impossible to observe the structure of the intermediate 2-nitrophenylnitrene, although a trace amount of the nitrene was observed in the IR spectra after photo-irradiation. In order to observe the structure of arylnitrene directly, several arylazide derivatives were prepared and the crystal structures were analyzed before and after photo-irradiation (Takayama *et al.*, 2010). Most derivatives were non-reactive or decomposed after photo-irradiation because the structural changes were too large to keep the single-crystal form. Only 2-azidobiphenyl was still crystalline after photo-irradiation; the structure of its product, 2-biphenylnitrene, was successfully analyzed by X-rays [see Scheme (II*b*)]. However, it was very difficult to observe the precise nitrene structure, because the 2-biphenylnitrene produced and the reactant 2-azidobiphenyl are superimposed in the crystal structure after photo-irradiation.

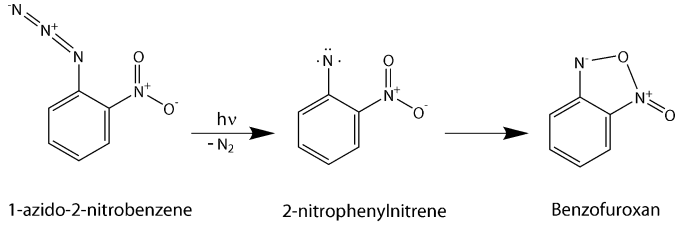

(*a*)

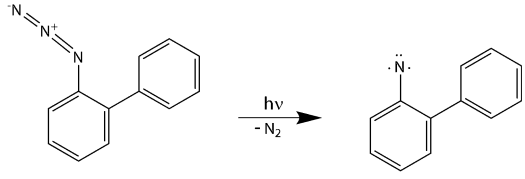

(*b*)

(II)

The above results suggested that if the acid–base complex crystals between the arylazides and dibenzylamines could be prepared, the photo-reaction should proceed with retention of the single-crystal form. This idea has already been applied in the crystalline-state photo-reactions of cobaloxime complexes (Ohashi & Hashizume, 1998; Hashizume & Ohashi, 1998, 1999), in which the carboxyl group was introduced to the axial base of the cobaloxime complexes and the dibenzylamine or dicyclohexylamine was used as a base compound and the acid–base complexes were formed between them. Three advantages for the acid–base complex formation are considered as follows:

(i) the crystallinity should be kept during the reaction, because the cavity around the reactive group may be

expanded compared with that of the crystal of just the reactant molecule;

(ii) the light can penetrate into the complex crystal more deeply than into the crystal of just the reactant molecule because the base amine may play the role of reaction matrix;

(iii) crystals suitable for X-ray studies may be easily obtained, because the phenyl or cyclohexyl group of the amines may improve the crystallinity.

In a previous paper (Kawano *et al.*, 2003) we reported the preliminary structure analysis of the triplet 3-carboxyphenylnitrene photo-produced from the acid–base complex of 3-azidobenzoic acid and dibenzylamine at 25 K, using synchrotron radiation at SPring-8. The N—C bond distance between the nitreno and the phenyl ring was observed to be 1.34 (4) Å, which is in good agreement with the theoretical calculation at the CASSCF(6,6)/6-31G* level, 1.343 Å.

In order to study the reaction pathways more extensively, a variety of acid–base complex crystals were prepared, using 2-azidobenzoic acid (2*a*), 3-azidobenzoic acid (3*a*) and 4-azidobenzoic acid (4*a*) as acids and dibenzylamine (db), *N*-benzyl-2-phenylethylamine (bp) and dicyclohexylamine (dc) as bases, which are shown in Scheme (III).

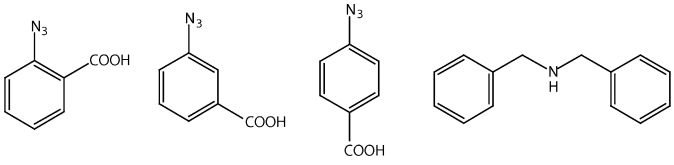

(III)

This paper shows the various reaction pathways of the photo-produced arylnitrenes in different crystal environments and illuminates the reaction mechanism.

2. Experimental

2.1. Preparation of azidobenzoic acids

2.1.1. 2-Azidobenzoic acid. 2-Aminobenzoic acid (2.10 g, 15.3 mmol) and sodium nitrite (1.13 g, 16.4 mmol) were dissolved in water (25 cm^3) with hydrochloric acid (7.5 cm^3) at 278 K. The solution was stirred for 1 h. Sodium azide (1.05 g, 16.2 mmol) in water (15 cm^3) was added at room temperature and stirred for 30 min. The mixture was filtered to give a white mousse, the crude product (1.19 g, 7.30 mmol).

2.1.2. 3-Azidobenzoic acid. 3-Aminobenzoic acid (2.10 g, 15.3 mmol) and sodium nitrite (1.13 g, 16.4 mmol) were dissolved in water (25 cm^3) with hydrochloric acid (7.5 cm^3) at 278 K. The solution was stirred for 1 h. Sodium azide (1.05 g, 16.2 mmol) in water (15 cm^3) was added at room temperature and stirred for 30 min. The mixture was filtered to give a white mousse, the crude product (2.19 g, 13.4 mmol).

2.1.3. 4-Azidobenzoic acid, dibenzylamine, *N*-benzyl-2-phenylethylamine and dicyclohexylamine. The compounds were obtained from a commercial source (Tokyo Kasei, Inc.).

2.2. Preparation of the acid–base complexes

An equimolar mixture of the component compounds was dissolved in methanol. After filtration, the solution was evaporated under reduced pressure until crude crystals were deposited.

2.2.1. 2-Azidobenzoic acid–dibenzylamine (2*a*-db). The pale-yellow crystals were obtained from toluene solution under a hexane atmosphere.

2.2.2. 3-Azidobenzoic acid–dibenzylamine [(3*a*-db-I) and (3*a*-db-II)]. The pale yellow crystals of forms (I) and (II) were obtained from diethyl ether solution. It was difficult to discriminate between the two forms without X-ray diffraction since their shapes and colors are nearly the same. Conditions for obtaining the two forms separately have not yet been worked out.

2.2.3. 3-Azidobenzoic acid–dicyclohexylamine (3*a*-dc). Pale yellow crystals were obtained from ethanol solution.

2.2.4. 4-Azidobenzoic acid–*N*-benzyl-2-phenylethylamine (4*a*-bp). Pale yellow crystals were obtained from toluene solution under a hexane atmosphere.

2.2.5. 4-Azidobenzoic acid–dibenzylamine [(4*a*-db-I) and (4*a*-db-II)]. The pale yellow crystals of forms (I) and (II) were obtained from toluene solution under a hexane atmosphere. Form (I) block-shaped crystals were obtained at an early stage and form (II) needle-shaped crystals were obtained after the form (I) crystals were removed.

2.2.6. 4-Azidobenzoic acid–dicyclohexylamine (4*a*-dc). Pale yellow crystals were obtained from ethanol solution.

No crystals suitable for X-ray analysis were obtained for (2*a*-dc), (2*a*-bp) and (3*a*-bp).

2.3. Spectroscopy and diffraction from the powdered acid–base complexes

2.3.1. FT-IR spectra. The FT-IR spectra were recorded in the rapid scan mode with an Excalibur FTS 3000 instrument (Bio-Rad). Powdered samples dispersed in KBr pellets were attached to the cold finger of an He cryogenic refrigerator system (DAIKIN PS24SS). The samples were irradiated with a high-pressure Hg lamp (SAN-EI UVF-352S, 350 W) in combination with a filter (L42 or L39 Toshiba, $\lambda > 420$ and > 390 nm) through the double KBr windows of the temperature-controlled cell at 80 K. All samples were measured at 80 K.

2.3.2. ESR spectra. The ESR spectra from powdered samples were recorded on a JES TE-200 (Jeol) spectrometer equipped with liquid He cryostat at 80 K. The samples were irradiated with a high-pressure Hg lamp (SAN-EI UVF-352S) in combination with a filter (L39 Toshiba).

2.3.3. Powder diffraction. In order to check whether or not the expected crystal modification had been obtained, powder diffraction patterns of the powdered samples used for spec-

troscopic measurements were measured with a Rigaku RINT-2400 diffractometer.

2.4. Single-crystal X-ray diffraction analysis

2.4.1. Data collection and reduction. Graphite-monochromated Mo $K\alpha$ radiation (λ = 0.71073 Å) was used with a Rigaku rotating anode X-ray generator (50 kV, 250 mA) and the temperature was controlled by a Rigaku cryostat system. All the diffraction data were collected by four sets of ω scans (−32 to 146.2°, 0.3° per frame) with χ = 54.83°, φ = 0, 90, 180 and 270° for each set using a Bruker SMART-CCD diffractometer (Siemens, 1995), except (4*a*-db-II). These data frames were integrated using the *SAINT* (Bruker, 2007) program package. Empirical absorption corrections were calculated using *SADABS* (Bruker, 2004*a*) and space groups were determined using *XPREP* (Bruker, 2004*b*). For (4*a*-db-II) the diffraction data were collected on a Rigaku R-AXIS RAPID diffractometer on 65 oscillation photographs (each oscillation angle was 4° with a 0.5° overlap margin) in the range $3.04 < \theta < 27.49°$. An empirical absorption correction was calculated using the *ABSCOR* program (Higashi, 1995) and the space group was determined with *TEXSAN* (Molecular Structure Corporation, 1999).

2.4.2. Photo-irradiation. The single crystal, which was rotated slowly on the diffractometer, was cooled using the cold-nitrogen gas-flow method to 80 K and was photo-irradiated using the light-guide tube from a high-pressure Hg lamp (SAN-EI UVF-352S, 350 W), the top of the tube being 7 cm from the crystal. Light with wavelengths longer than 390 or 420 nm was used by inserting a filter (L39 or L42 Toshiba) between the top of the tube and the crystal. As the crystals gradually decomposed over the course of the photo-irradiation, the rocking curves and shapes of several diffraction peaks were monitored. Photo-irradiation was stopped before the crystallinity was significantly degraded. The exposure time, temperature and filters used were as follows; 2 h, 88 K and L39 for (2*a*-db), 11 h, 80 K and L42 for (3*a*-db-I), 10 h, 80 K and L42 for (3*a*-db-II), 11 h, 82 K and L42 for (3*a*-dc), 6 h, 92 K and L42 for (4*a*-dp), 32 h, 88 K and L42 for (4*a*-bp-I). The temperature was controlled to within a deviation of 2 K. The diffractometer was covered with black sheets to shut out room light during data collection and photo-irradiation.

2.5. Structure refinement

2.5.1. Crystals before photo-irradiation. Every structure was solved by direct methods (*SHELXS*97; Sheldrick, 2008) and refined by full-matrix least-squares (*SHELXL*97; Sheldrick, 2008). All non-H atoms were refined anisotropically. All H atoms were located in the difference-Fourier map and refined isotropically.

2.5.2. Crystals after photo-irradiation. To compare the molecular structures before and after photo-irradiation, X-ray data after photo-irradiation were collected using the same crystal at the same temperature as those before photo-irradiation. The initial molecular structures of non-H atoms were treated as two rigid groups in which their displacement parameters were refined anisotropically. One pivot atom was applied for the azidobenzoic acid molecule and the other was for the amine molecule. The rigid groups were allowed to rotate and translate. No large residual peak appeared around the amine molecule, but new residual peaks and holes appeared in the vicinity of the azido moiety. The peaks were assigned to a dinitrogen molecule. The other residual peaks appeared around azidobenzoic acid, which indicated that the azidobenzoic acid underwent a chemical reaction. The isotropic displacement factors of the N atoms of the dinitrogen molecule were constrained to have the same value. The refinement of the original azide molecule and the new photo-products were performed alternately, such that one was refined with a rigid-body model if the other was refined with restraints. The bond distances, bond angles and anisotropic displacement parameters of the azide molecule and arylnitrene were restrained to have the same values as the corresponding ones of the original molecule. At the final stage the parameters of arylnitrene and dinitrogen were refined with restraints and those of the azide molecule were refined with the rigid-body model. The occupancy factors of the dinitrogen and product molecules were constrained to x and y, where $1 - x$ and $1 - y$ are the occupancy factors of the initial azido moiety and benzoic acid. If the parameters of x and y converged to different values, the arylnitrene molecule with an occupancy factor of $x - y$ was assumed to be completely superimposed on the initial azidobenzoic acid molecule or to have random orientations around the initial azidobenzoic acid molecule. All H atoms were located geometrically. There are no peaks higher than 0.30, 0.30, 0.57, 0.40 and 0.30 e Å^{-3} in the final difference electron-density maps of (2*a*-db), (3*a*-db-I), (3*a*-db-II), (3*a*-dc) and (4*a*-bp).

For the (4*a*-db-I) crystal attempts to analyze the appropriate structure after photo-irradiation have been unsuccessful, because the difference electron-density map showed no significant change owing to dinitrogen formation, although the unit-cell volume expanded from 2581.3 (2) to 2671.1 (3) Å^3 and the three-dimensional intensity data were successfully collected after photo-irradiation. Since this crystal has two crystallographically independent 4-azidobenzoic molecules, *A* and *B*, in an asymmetric unit, some complicated structural change other than nitrene formation may occur during photo-irradiation.

Since the (4*a*-db-II) single crystal was too thin to measure by X-ray diffraction, only data collection before photo-irradiation was performed. Photo-irradiation on the (4*a*-db-II) crystal was not carried out. The (4*a*-dc) crystal was photo-irradiated on the diffractometer at 80 K. The crystal decomposed within 2 h after photo-irradiation. Intensity data collection was not attempted for the (4*a*-dc) crystal.

3. Results

3.1. Molecular and crystal structures before photo-irradiation

The crystal data and experimental details of five arylazide acid–base complex crystals, (2*a*-db), (3*a*-db-I), (3*a*-db-II), (3*a*-

Table 1
Experimental details of the complex crystals before photo-irradiation.

Experiments were carried out with Mo $K\alpha$ radiation.

	(2*a*-db-I)	(3*a*-db-I′)	(3*a*-db-II′)	(3*a*-dc′)	(4*a*-bp′)
Crystal data					
Chemical formula	$C_{21}H_{20}N_4O_2$	$C_{21}H_{20}N_4O_2$	$C_{21}H_{20}N_4O_2$	$C_{19}H_{28}N_4O_2$	$C_{22}H_{22}N_4O_2$
M_r	360.41	360.41	360.41	344.45	374.44
Crystal system, space group	Monoclinic, *Cc*	Orthorhombic, $P2_12_12_1$	Monoclinic, $P2_1/c$	Triclinic, $P\bar{1}$	Triclinic, $P\bar{1}$
Temperature (K)	88	80	78	82	92
a, *b*, *c* (Å)	19.9575 (7), 10.0329 (3), 9.9849 (3)	8.9705 (1), 14.4208 (1), 14.8689 (2)	10.854 (2), 8.666 (2), 21.081 (4)	9.1925 (5), 10.1813 (5), 11.3543 (6)	8.0615 (2), 10.3615 (2), 13.5356 (4)
α, β, γ (°)	90, 106.640 (2), 90	90, 90, 90	90, 104.51 (3), 90	110.816 (1), 103.168 (2), 103.370 (1)	72.503 (1), 72.933 (1), 70.506 (1)
V (Å^3)	1915.57 (11)	1923.47 (4)	1919.7 (7)	908.51 (8)	992.76 (4)
Z	4	4	4	2	2
μ (mm^{-1})	0.08	0.08	0.08	0.08	0.08
Crystal size (mm)	0.41 × 0.34 × 0.22	0.40 × 0.20 × 0.15	0.31 × 0.16 × 0.12	0.44 × 0.38 × 0.26	0.31 × 0.21 × 0.08
Data collection					
Diffractometer	Bruker SMART CCD area detector system	Bruker SMART CCD area detector system	Bruker SMART CCD area detector system	Bruker SMART CCD area detector system	Bruker SMART CCD area detector system
Absorption correction	Empirical (using intensity measurements) using *SADABS*	Empirical (using intensity measurements) using *SADABS*	Empirical (using intensity measurements) using *SADABS*	Empirical (using intensity measurements) using *SADABS*	Empirical (using intensity measurements) using *SADABS*
T_{min}, T_{max}	0.967, 0.982	0.968, 0.988	0.975, 0.990	0.964, 0.979	0.975, 0.993
No. of measured, independent and observed [$I > 2\sigma(I)$] reflections	14 815, 2788, 2668	30 731, 3163, 2908	29 789, 5594, 4774	14 513, 5259, 4561	15 962, 5766, 4057
R_{int}	0.035	0.038	0.034	0.023	0.053
Refinement					
$R[F^2 > 2\sigma(F^2)]$, $wR(F^2)$, S	0.027, 0.073, 1.11	0.030, 0.081, 1.17	0.036, 0.100, 1.05	0.034, 0.100, 1.06	0.050, 0.148, 1.03
No. of reflections	2788	3163	5594	5259	5766
No. of parameters	306	324	306	312	319
No. of restraints	2	0	0	0	0
H-atom treatment	Only H-atom coordinates refined	Only H-atom coordinates refined	Only H-atom coordinates refined	Only H-atom coordinates refined	Only H-atom coordinates refined
$\Delta\rho_{max}$, $\Delta\rho_{min}$ (e Å^{-3})	0.21, −0.17	0.25, −0.17	0.33, −0.22	0.35, −0.24	0.40, −0.26

Computer programs used: *SMART* (Siemens, 1995), *PROCESS-AUTO* (Rigaku, 1995), *SHELXS*97, *SHELXL*97, *SHELXTL*97 (Sheldrick, 2008), *SAINT* (Bruker, 2007), *SADABS* (Bruker, 2004*a*), *TEXSAN* (Molecular Structure Corporation, 1999), *ORTEP*3 for Windows (Farrugia, 1997).

dc) and (4*a*-bp), before photo-irradiation are summarized in Table 1. The crystal data and experimental details of the other three crystals before photo-irradiation have been deposited in Table S1.[1] Since the H atom of the benzoic acid is transferred to the amine in all crystals, the azidobenzoate and ammonium salt make a fairly strong hydrogen bond of $(-COO)^-$—$(>NH_2)^+$ between them.

The molecular structure of (2*a*-db) is shown in Fig. 1(*a*) and the crystal structure is shown in Fig. 1(*b*). The azido group is approximately coplanar with the benzene ring, the torsion angle of C2—C1—N1—N2 being 8.9 (2)°. On the other hand, the carboxyl group is not coplanar with the benzene ring to avoid the short contact with the azido group, the dihedral angle between the carboxyl group and the benzene ring being 38.0 (2)°. Molecules (2*a*) and (db) are connected with two CO···HN hydrogen bonds and create a one-dimensional chain along the *c* axis connected by the glide plane. The O1···N4 and O2···N4 distances are 2.709 (1) and 2.731 (1) Å, and N4—H01···O1 and N4—H02···O2 angles are 172 (2) and 179 (2)°.

The molecular and crystal structures of (3*a*-db-I) are shown in Figs. 2(*a*) and (*b*), respectively, which are essentially the same as those analyzed using the data observed at 25 K at SPring-8 (Kawano *et al.*, 2003). The azido and carboxyl groups are nearly coplanar with the benzene ring, the torsion angle of C2—C1—N1—N2 and dihedral angles of carboxyl group being 9.7 (2) and 8.8 (2)°. The (3*a*) and (db) molecules are connected with two CO···HN hydrogen bonds and create a one-dimensional chain along the *a* axis connected by a twofold screw axis. The O1···N4 and O2···N4 distances are 2.667 (1) and 2.735 (1) Å, and the N4—H01···O1 and N4—H02···O2 angles are 166 (2) and 168 (2)°. The azido groups are connected by another twofold screw axis along the *a* axis.

The molecular and crystal structures of (3*a*-db-II) are shown in Figs. 3(*a*) and (*b*). Although the azido and carboxyl groups are approximately coplanar with the benzene ring, the azido group takes the opposite conformation to that of (3*a*-db-I). The torsion angle of C6—C1—N1—N2 and dihedral angles

[1] Supplementary data for this paper are available from the IUCr electronic archives (Reference: OG5043). Services for accessing these data are described at the back of the journal.

are 14.2 (1) and 13.4 (1)°. The (3*a*) and (db) molecules are connected by two CO···HN hydrogen bonds and create a one-dimensional chain along the *b* axis connected by a twofold screw axis. The O1···N4 and O2···N4 distances are 2.723 (1) and 2.710 (1) Å, and the N4—H01···O1 and N4—H02···O2 angles are 162 (1) and 165 (1)°. The closest azido groups are connected by an inversion center.

The molecular and crystal structures of (3*a*-dc) are shown in Figs. 4(*a*) and (*b*). The azido and carboxyl groups are approximately coplanar with the benzene ring, the torsion angle of C2—C1—N1—N2 and dihedral angles being 5.4 (1) and 7.1 (1)°. Both the cyclohexyl groups are in stable chair forms. The (3*a*) and (dc) molecules are connected with two CO···HN hydrogen bonds and make a dimer around an inversion center. The O1···N4 and O2···N4 distances are 2.7888 (8) and 2.7194 (8) Å, and the N4—H41···O1 and N4—H42···O2 angles are 166 (1) and 165 (1)°. The closest intermolecular contact between azido groups is across another inversion center.

The molecular and crystal structures of (4*a*-bp) are shown in Figs. 5(*a*) and (*b*). The alkyl group of the amine is in the *trans* conformation. The azido and carboxyl groups are almost coplanar, the torsion angle of C2—C1—N1—N2 and dihedral angles being 9.4 (2) and 18.7 (2)°. The (4*a*) and (bp) molecules are connected by two CO···HN hydrogen bonds and make a dimer around an inversion center. The O1···N4 and O2···N4 distances are 2.669 (1) and 2.691 (2) Å, and the N4—H01···O1 and N4—H02···O2 angles are 158 (1) and 160 (1)°. The closest intermolecular contact between azido groups is across another inversion center.

The molecular and crystal structures of (4*a*-db-I), (4*a*-db-II) and (4*a*-dc) are are included in Figs. S1, S2 and S3 of the supplementary material.

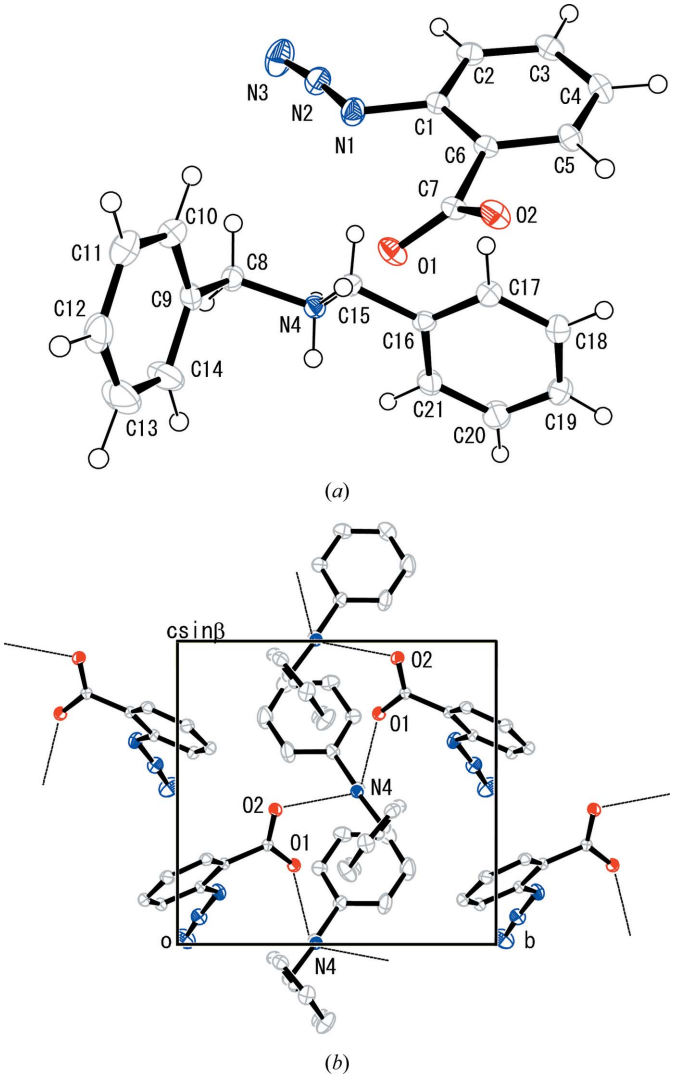

Figure 1
(*a*) Molecular structure of (2*a*-db) and (*b*) the crystal structure viewed along the *c* axis before photo-irradiation. The displacement ellipsoids are drawn at the 50% probability level. The circles of the H atoms are drawn on an arbitrary scale. The dotted lines indicate the intermolecular hydrogen bonds.

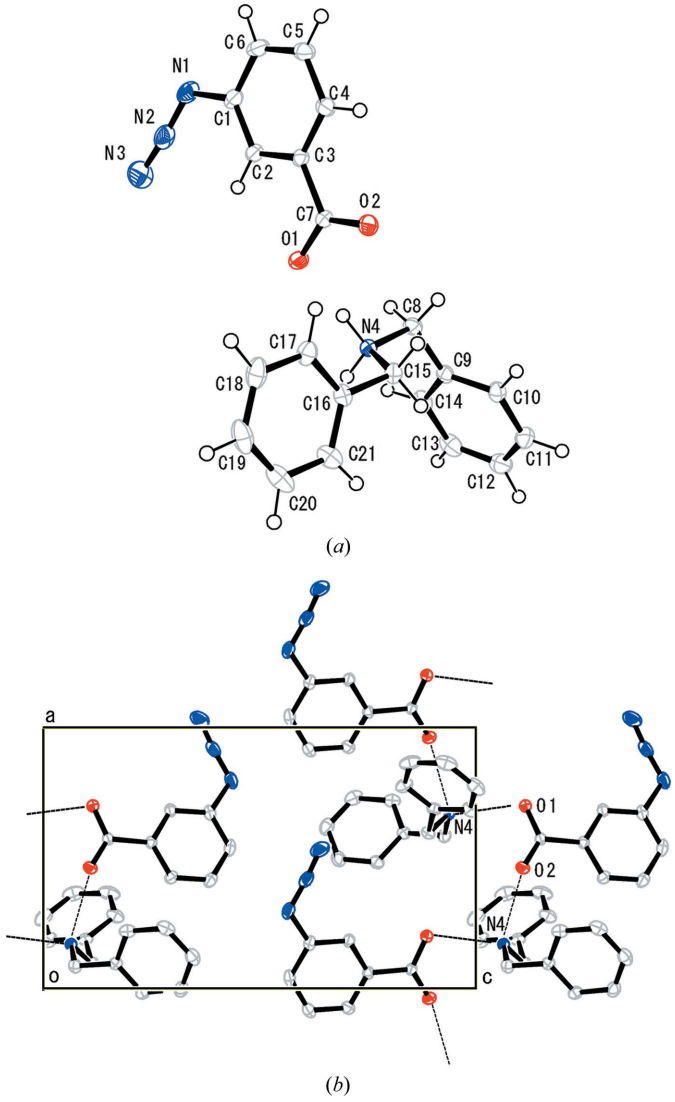

Figure 2
(*a*) Molecular structure of (3*a*-db-I) and (*b*) the crystal structure viewed along the *a* axis before photo-irradiation. The displacement ellipsoids are drawn at the 50% probability level. The circles of the H atoms are drawn on an arbitrary scale. The dotted lines indicate intermolecular hydrogen bonds.

3.2. IR studies

The IR spectra of the powdered crystals were measured including azacycloheptatetraene which was produced in the photo-reaction process. The difference IR spectra of five crystals, (2*a*-db), (3*a*-db-I), (3*a*-db-II), (3*a*-dc) and (4*a*-bp), before and after photo-irradiation are shown in Fig. 6. Although the absorption bands for the azido group (around 2130 cm^{-1}) disappeared in all the crystals, the new band at 1870 cm^{-1} only appeared in (3*a*-db-I), (3*a*-db-II) and (3*a*-dc) crystals. These new bands were assigned to azacycloheptatetraene (Chapman & Roux, 1978; Dyall & Kemp, 1967). Since the azacycloheptatetraene produced may be unstable and only a small portion of the azidobenzoic acid undergoes a photo-reaction in a single crystal, it is difficult to analyze the precise structure of azacycloheptatetraene in the structure after photo-irradiation.

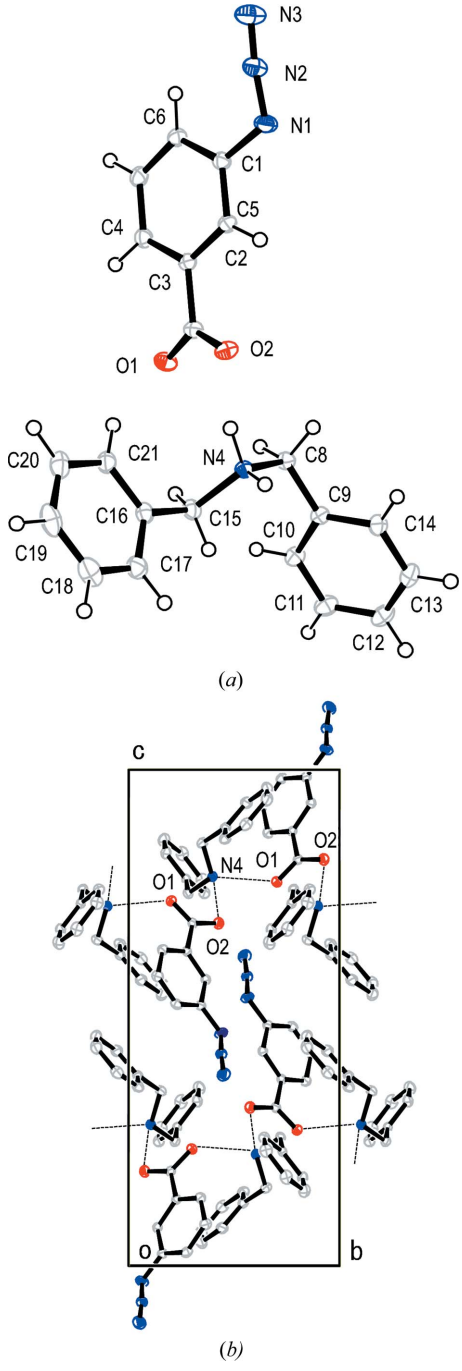

Figure 3
(*a*) Molecular structure of (3*a*-db-II) and (*b*) the crystal structure viewed along the *b* axis before photo-irradiation. The displacement ellipsoids are drawn at the 50% probability level. The circles of the H atoms are drawn on an arbitrary scale. The dotted lines indicate intermolecular hydrogen bonds.

3.3. ESR studies

The ESR spectra of the powdered crystals were taken to check for the formation of the triplet arylnitrene. The most stable triplet arylnitrene has an $sp^2px^1py^1$ orbital state (Kim *et al.*, 1992; Hrovat *et al.*, 1992). Before photo-irradiation, no signals were observed for any crystal. The ESR spectra of (2*a*-db), (3*a*-db-I), (3*a*-db-II), (3*a*-dc) and (4*a*-bp) after photo-irradiation at 80 K are shown in Fig. 7. The characteristic strong triplet signal was observed around 680 mT (Smolynsky *et al.*, 1962; Chapman *et al.*, 1978). This means that the triplet

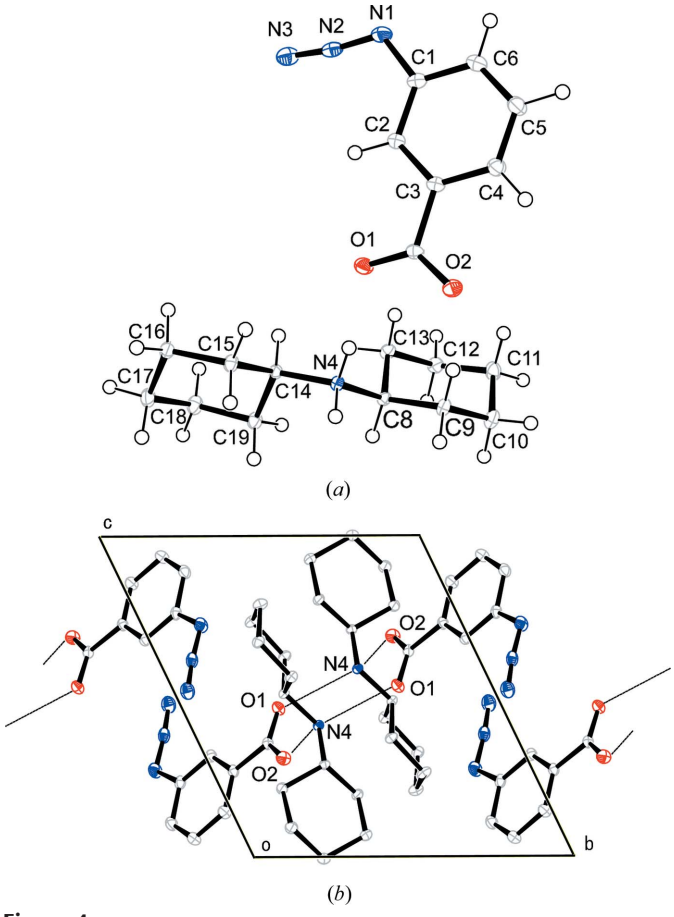

Figure 4
(*a*) Molecular structure of (3*a*-dc) and (*b*) the crystal structure viewed along the *a* axis before photo-irradiation. The displacement ellipsoids are drawn at the 50% probability level. The circles of the H atoms are drawn on an arbitrary scale. The dotted lines indicate intermolecular hydrogen bonds.

arylnitrene was photo-produced in every crystal. In (2*a*-db), (3*a*-dc) and (4*a*-bp) there are some peaks around the 330 mT field (Wasserman, 1971).

3.4. Molecular structures after photo-irradiation

The crystal data and experimental details of the five arylazide complex crystals after photo-irradiation, (2*a*-db′), (3*a*-db-I′), (3*a*-db-II′), (3*a*-dc′) and (4*a*-bp′), are summarized in Table 2. The same data for (4*a*-db-I′) are included in Table S1 of the supplementary material.

The difference electron-density maps of the (2*a*-db) crystal before and after photo-irradiation are shown in Figs. 8(*a*) and (*b*). Before photo-irradiation all the residual peaks can be interpreted as bonding electrons. After photo-irradiation, (2*a*-db′), new residual peaks and holes appeared in the vicinity of the azido and carboxyl groups. The former peaks were assigned to a dinitrogen molecule produced from the azido group. The latter peaks indicated that the nitreno group produced attacked the O atom of the carboxyl group to form a new molecule with the five-membered ring, that is, 2,1-benzisoxazolone. No significant change was found in the structure of (db). The disordered structure after photo-irradiation is shown in Fig. 8(*c*). The atoms with and without P correspond to the photo-produced and original atoms, respectively. The exocyclic C—O bond, C7P—O2P is 1.18 (4) Å, which indicates a double bond. This figure clearly indicates that the reaction proceeded as shown in Scheme (IV).

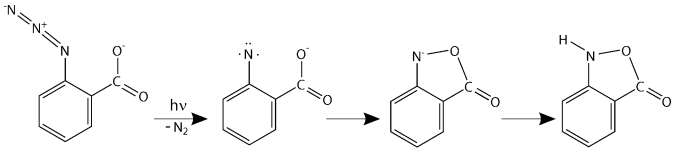

(IV)

Although little change was observed in the intermolecular hydrogen-bond distance of N···O for one of the hydrogen bonds, N4—H2···O2, a significant change was observed for another hydrogen bond, N4—H1···O1. The N4···O2F and N4F···O2P distances after photo-irradiation are 2.709 (2) and

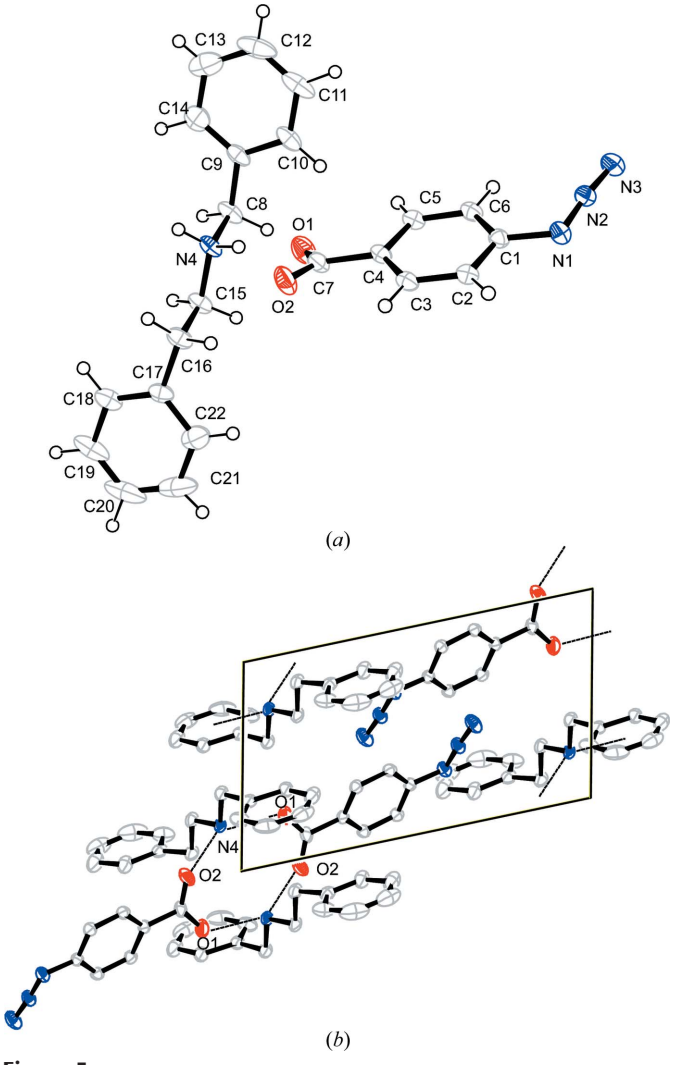

Figure 5
(*a*) Molecular structure of (4*a*-bp) and (*b*) the crystal structure viewed along the *b* axis before photo-irradiation. The displacement ellipsoids are drawn at the 50% probability level. The circles of the H atoms are drawn on an arbitrary scale. The dotted lines indicate intermolecular hydrogen bonds.

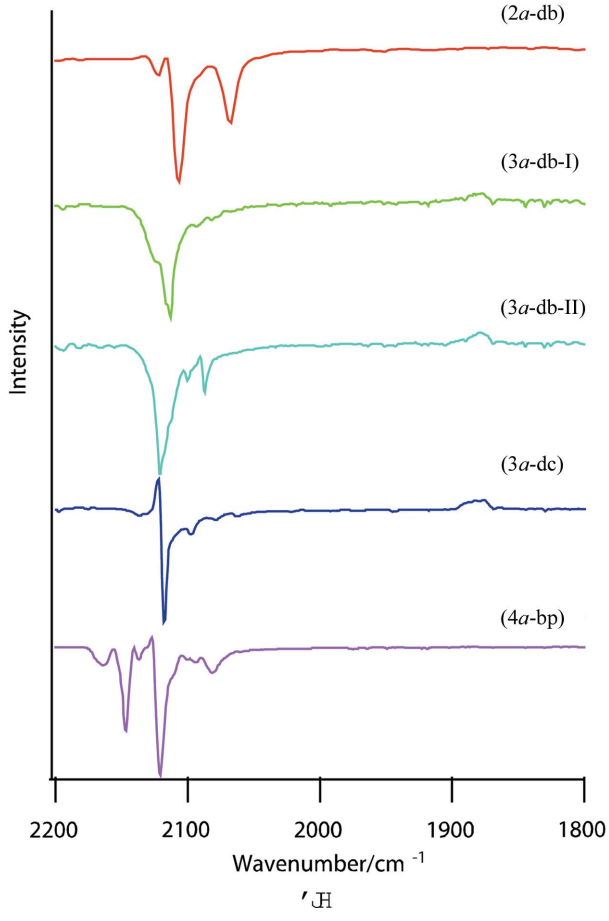

Figure 6
Difference IR spectra of five arylazide complexes, (2*a*-db), (3*a*-db-I), (3*a*-db-II), (3*a*-dc) and (4*a*-bp), dispersed in KBr matrices before and after photo-irradiation at 80 K.

Table 2
Experimental details of the complex crystals after photo-irradiation.

	(2*a*-db′)	(3*a*-db-I′)	(3*a*-db-II′)	(3*a*-dc′)	(4*a*-bp′)
Crystal data					
Chemical formula	$C_{21}H_{20}N_4O_2$	$C_{21}H_{20}N_4O_2$	$C_{21}H_{20}N_4O_2$	$C_{19}H_{28}N_4O_2$	$C_{22}H_{22}N_4O_2$
M_r	360.41	360.41	360.41	344.45	374.44
Crystal system, space group	Monoclinic, *Cc*	Orthorhombic, $P2_12_12_1$	Monoclinic, $P2_1/c$	Triclinic, $P\bar{1}$	Triclinic, $P\bar{1}$
Temperature (K)	88	80	82	82	92
a, *b*, *c* (Å)	19.892 (7), 9.966 (2), 10.068 (2)	8.9378 (2), 14.5133 (3), 14.9386 (3)	10.908 (2), 8.7884 (18), 21.240 (4)	9.2356 (4), 10.2844 (5), 11.3770 (6)	8.1100 (4), 10.3363 (6), 13.6177 (7)
α, β, γ (°)	90, 107.06 (4), 90	90, 90, 90	90, 104.87 (3), 90	111.073 (2), 103.254 (2), 103.553 (2)	72.377 (2), 73.542 (2), 70.583 (1)
V (Å^3)	1908.1 (9)	1937.79 (7)	1967.9 (7)	919.86 (8)	1004.67 (9)
Z	4	4	4	2	2
μ (mm^{-1})	0.08	0.08	0.08	0.08	0.08
Crystal size (mm)	0.41 × 0.34 × 0.22	0.40 × 0.20 × 0.15	0.31 × 0.16 × 0.12	0.44 × 0.38 × 0.26	0.31 × 0.21 × 0.08
Data collection					
Diffractometer	Bruker SMART CCD area detector system	Bruker SMART CCD area detector system	Bruker SMART CCD area detector system	Bruker SMART CCD area detector system	Bruker SMART CCD area detector system
Absorption correction	Empirical (using intensity measurements) using *SADABS*	Empirical (using intensity measurements) using *SADABS*	Empirical (using intensity measurements) using *SADABS*	Empirical (using intensity measurements) using *SADABS*	Empirical (using intensity measurements) using *SADABS*
T_{min}, T_{max}	0.967, 0.982	0.968, 0.988	0.975, 0.990	0.965, 0.979	0.975, 0.994
No. of measured, independent and observed [$I > 2\sigma(I)$] reflections	7279, 2723, 2511	30 720, 3183, 2575	30 460, 5734, 4338	14 760, 5328, 4342	16 229, 5842, 2789
R_{int}	0.042	0.050	0.044	0.023	0.069
Refinement					
$R[F^2 > 2\sigma(F^2)]$, $wR(F^2)$, S	0.046, 0.139, 1.02	0.059, 0.181, 1.06	0.067, 0.192, 1.06	0.049, 0.141, 0.90	0.079, 0.257, 0.99
No. of reflections	2723	3183	5734	5328	5842
No. of parameters	210	183	206	171	210
No. of restraints	3	0	5	1	9
H-atom treatment	H-atom parameters constrained	H-atom parameters constrained	H-atom parameters constrained	H atoms treated by a mixture of independent and constrained refinement	H-atom parameters constrained
$\Delta\rho_{max}$, $\Delta\rho_{min}$ (e Å^{-3})	0.37, −0.31	0.35, −0.24	0.57, −0.56	0.40, −0.46	0.39, −0.29

Computer programs used: see Table 1.

2.71 (3) Å, respectively, which are approximately the same as 2.731 (1) Å before photo-irradiation. The N4···O1 distance increased from 2.709 (1) to 2.714 (4) Å in the major portion, but the N4···N1P distance is 2.91 (3) Å in the minor portion. The N4···N1 distance is shorter than the sum of van der Waals radii after photo-irradiation. This means a new N—H···N hydrogen bond was created between N4 and N1. The H1 atom is transferred to the N1 atom and the hydrogen bond probably changed from $N4^+$—H1···$N1^-$ to N4···H1—N1, since the N atom of the five-membered ring should have a H atom, considering the C1P—N1P and O1P—N1P distances are 1.42 (4) and 1.34 (4) Å, which are single bond distances. The final photoproduct should be indicated as shown in Scheme (IV).

It must be emphasized that the unit-cell volume of (2*a*-db) decreased by 7.5 Å^3 after photo-irradiation, although those of the other crystals increased significantly after photo-irradiation. The size of the 2,1-benzisoxazolone produced is significantly smaller than that of the original 2-azidobenzoic acid. The cell volume shrinkage caused by the five-membered ring formation may overcome the expansion owing to the formation of the dinitrogen molecule from the azido group.

The occupancy factors of dinitrogen and 2,1-benzisoxazolone molecules are 0.131 (8) and 0.105 (5). The difference in occupancy [0.026 (9)] may indicate the existence of the intermediate 2-carboxyphenylnitrene, considering the ESR measurement which indicates the triplet arylnitrene, although the value may be within experimental error.

It was recently reported from the UV and IR spectra of 2-azidobenzoic acid crystalline samples that the heterocyclic ring of 2,1-benzisoxazolone was produced *via* the singlet arylnitrene and the dimer 2,2′-dicarboxyazobenzene was produced *via* the triplet arylnitrene (Budruev *et al.*, 2003). Since the nitreno group produced was too far from the neighboring nitreno group, as shown in Fig. 1(*b*), it was not dimerized to 2,2′-dicarboxyazobenzene in a single crystal after intersystem crossing from singlet to triplet.

For the (3*a*-db-I′) crystal the difference electron-density map is shown in Fig. 9(*a*). New residual peaks and holes appeared in the vicinity of the azido group. These peaks were

assigned to a dinitrogen molecule produced from the azido group. The occupancy factor of the dinitrogen molecule converged to 0.25 (2). The disordered structure after photo-irradiation is shown in Fig. 9(*b*). Since the original 3-azidobenzoic acid and 3-carboxyphenylnitrene produced almost overlap each other, it was impossible to separate the two molecules. However, the photo-produced structure is essentially the same as that analyzed using the intensity data collected at the BL02B1 station of SPring-8 at 25 K, although the occupancy factor of the dinitrogen molecule was 0.075 at 25 K (Kawano *et al.*, 2003). The intermolecular hydrogen bonds of N4···O1 and N4···O2 fix the carboxyl group of the benzoic acid tightly to the dibenzylamines at 25 K. The 3-carboxyphenylnitrene produced was slightly shifted from the original position of the 3-azidobenzoic acid owing to steric repulsion with the dinitrogen molecule produced, as shown in Fig. 9(*c*). The C1—N1(nitrene) bond was successfully analyzed to be 1.34 (4) Å. The closest arylazides are related by a twofold screw axis so that the azido group is surrounded with inert phenyl rings of adjacent molecules, as shown in Fig. 2(*b*). The intermolecular distance between the closest N1 atoms is 5.782 (2) Å in the structure before photo-irradiation. There is

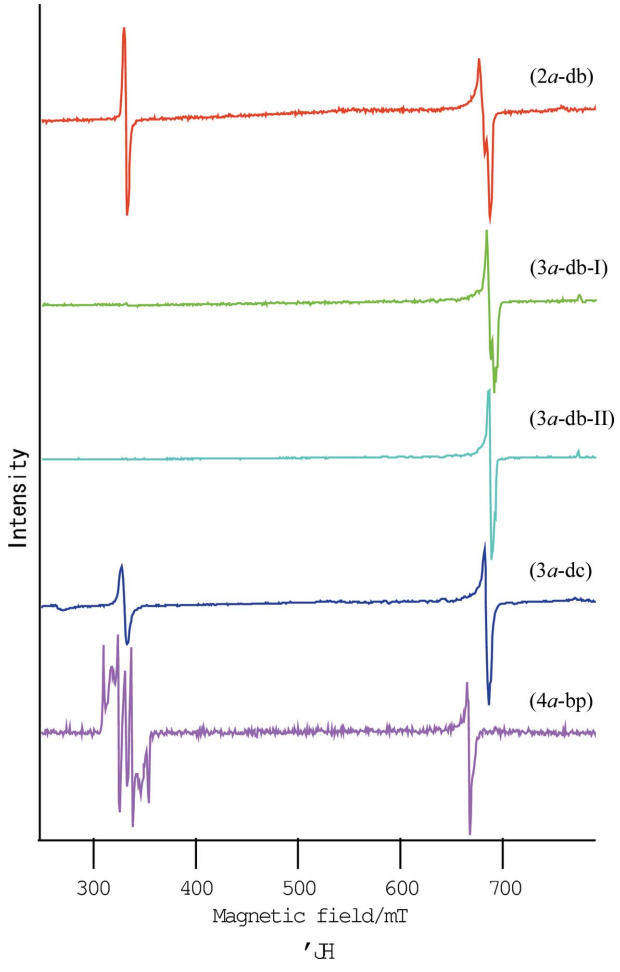

Figure 7
ESR spectra of five arylazide complexes, (2*a*-db), (3*a*-db-I), (3*a*-db-II), (3*a*-dc) and (4*a*-bp), after photo-irradiation at 80 K.

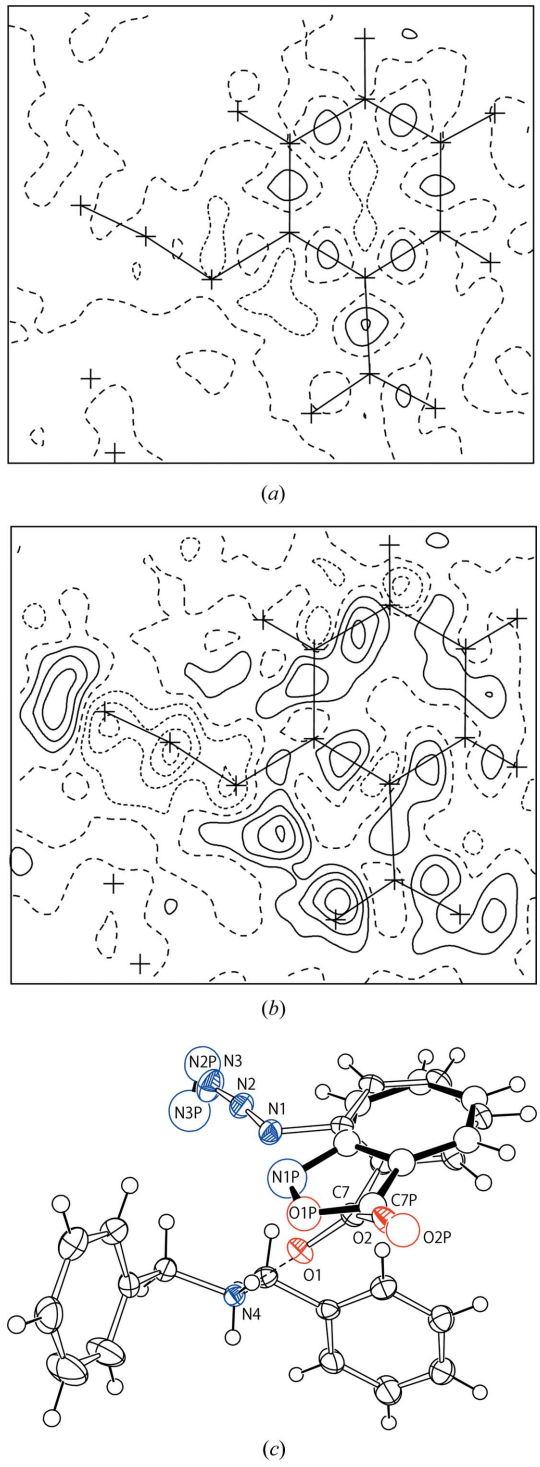

Figure 8
Difference electron-density maps of (2*a*-db) (*a*) before photo-irradiation and (*b*) after photo-irradiation, projected on the 2-azidobenzoic acid. In these two cases the calculated electron density of the original molecule before photo-irradiation was subtracted from the observed densities. Solid and dashed lines indicate positive and negative electron densities drawn every 0.1 e Å^{-3}. (*c*) Disordered molecular structure after photo-irradiation. The open bonds indicate the original molecules, the atomic positions with F character have slightly different positions from the original ones. The atoms with P character appeared at the new positions. The molecule with the black bonds is newly produced. The displacement ellipsoids are drawn at the 50% probability level and the circles of the H atoms are drawn on an arbitrary scale.

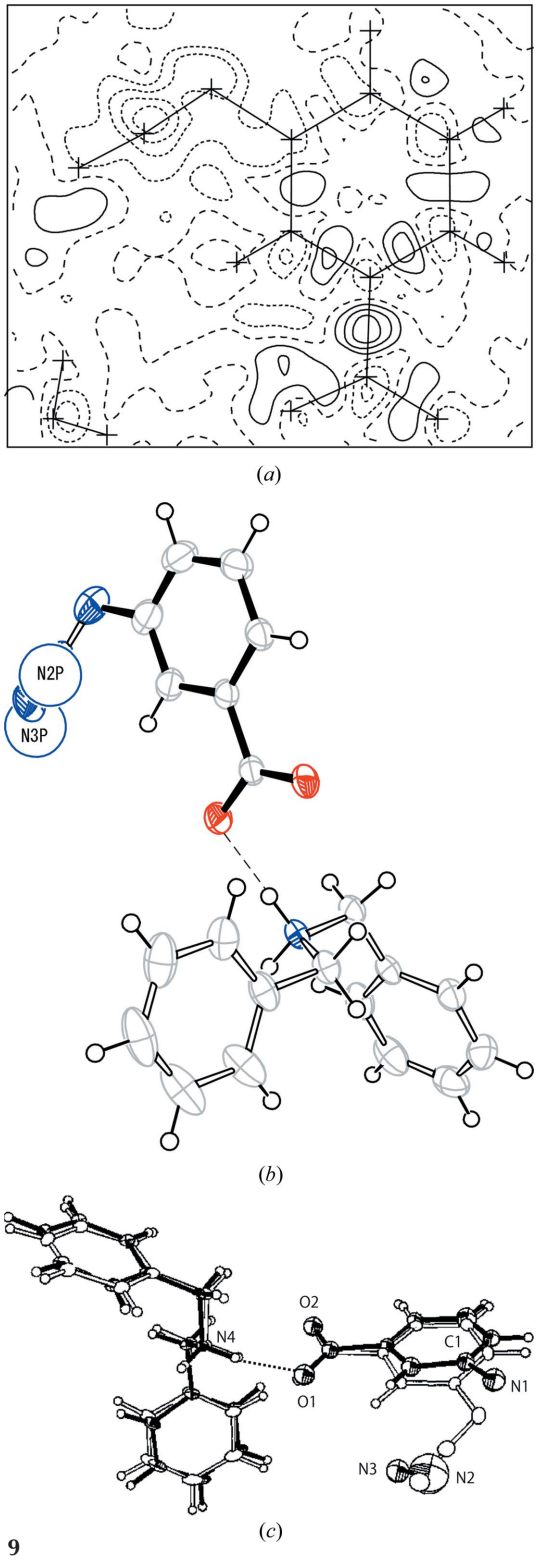

Figure 9
(*a*) Difference electron-density map of (3*a*-db-I) on the plane of 3-azidobenzoic acid; the density calculated using atomic positions before photo-irradiation was subtracted from the observed one. Solid and dashed lines indicate the positive and negative electron densities drawn every 0.1 e Å^{-3}. (*b*) Molecular structure after photo-irradiation. The open bonds indicate the original molecules. The molecule with the black bonds is the newly produced arylnitrene. However, it was impossible to separate the atoms of 3-carboxyphenylnitrate from 3-azidobenzoic acid. (*c*) Disordered molecular structure (3*a*-db-I) at 25 K whose data were collected at SPring-8.

no possibility for the 3-carboxyphenylnitrene produced to make a dimer with the neighboring one. This is the reason why the unstable nitrene can be observed in the crystal after photo-irradiation.

For the (3*a*-db-II′) crystal the difference electron-density map is shown in Fig. 10(*a*). New residual peaks and holes appeared in the vicinity of the azido group, which were assigned to a dinitrogen molecule from the azido group. Moreover, new peaks appeared between 3-azidobenzoic acid molecules related by an inversion. The two photo-produced 3-carboxyphenylnitrenes came close to each other and a dimer, 3,3′-dicarboxy-*trans*-azobenzene, was formed. The disordered structure after photo-irradiation is shown in Fig. 10(*b*). The intermolecular distance between the N1 atoms related by an inversion center [4.067 (2) Å] before photo-irradiation is shorter than in (3*a*-db-I). After photo-irradiation, the N1P—N1P′ distance became 1.29 (7) Å, which is the N═N double bond. The hydrogen bonds of N4···O1 and N4···O2 before irradiation, 2.723 (1) and 2.710 (1) Å, became 2.66 (3) and 2.45 (3) Å. It is clear that the crystal packing around the arylnitrene produced plays an important role in the reaction pathway. The occupancy factors are 0.177 (4) for the dinitrogen molecule and 0.074 (4) for 3,3′-dicarboxy-*trans*-azobenzene. The ESR spectra indicated the existence of the triplet arylnitrene. This means the triplet 3-carboxyphenylnitrene with an occupancy factor of 0.103 (6) is overlapped with the original 3-azidobenzoic acid molecule or may have a random orientation. Although the IR spectra also indicated the existence of azacycloheptatetraene, it was impossible to assign the azacycloheptatetraene molecule in the difference electron density map since it may be completely buried in the disordered structure of arylazide, arylnitrene and azobenzene, if present at all.

For the (3*a*-dc′) crystal the difference electron-density maps are shown in Fig. 11(*a*). New peaks and holes appeared in the vicinity of the azido group. These were assigned to a dinitrogen molecule produced from the azido group. The structure was refined to a disordered one composed of the original complex between 3-azidobenzoic acid and dicyclohexylamine, and the photoproducts, dinitrogen and 3-carboxyphenylnitrene, as shown in Fig. 11(*b*), in which the nitrene is completely overlapped with the benzoic acid. The occupancy factor of the dinitrogen molecule is 0.183 (4). The distance of the closest nitreno groups related by the inversion center is too long, 5.890 (1) Å, to make a dimer. The intermolecular hydrogen bonds of N4···O1 and N4···O2 before irradiation, 2.7888 (8) and 2.7194 (8) Å, are almost the same as those after photo-irradiation, 2.783 (1) and 2.727 (1) Å.

For the (4*a*-bp′) crystals the difference electron-density map is shown in Fig. 12(*a*). New peaks appeared in the vicinity of the two azido groups related by an inversion. These peaks were assigned to the central N═N bond of 4,4′-dicarboxy-*trans*-azobenzene and two dinitrogen molecules, as shown in Fig. 12(*b*). The center of the N═N bond of 4,4′-dicarboxy-*trans*-azobenzene is situated on the crystallographic inversion center. Two 4-azidobenzoic acids contact each other around an inversion center, which is the closest one. The intermolecular

distance between the closest N1 atoms to the inversion center, 3.411 (2) Å, before photo-irradiation is shorter than that of (3*a*-db-II). After photo-irradiation, the N1P—N1P′ bond became 1.33 (4) Å, which is an N═N double bond. The intermolecular hydrogen bonds of N4···O1 and N4···O2 before photo-irradiation are 2.669 (1) and 2.691 (2) Å, which are somewhat different from the distances after photo-irradiation, 2.52 (2) and 2.71 (2) Å. Such differences may be caused by an N═N bond formation in the opposite site of the benzene rings.

The occupancy factor for 4,4′-dicarboxy-*trans*-azobenzene became 0.149 (4), but the factor for dinitrogen was 0.088 (5).

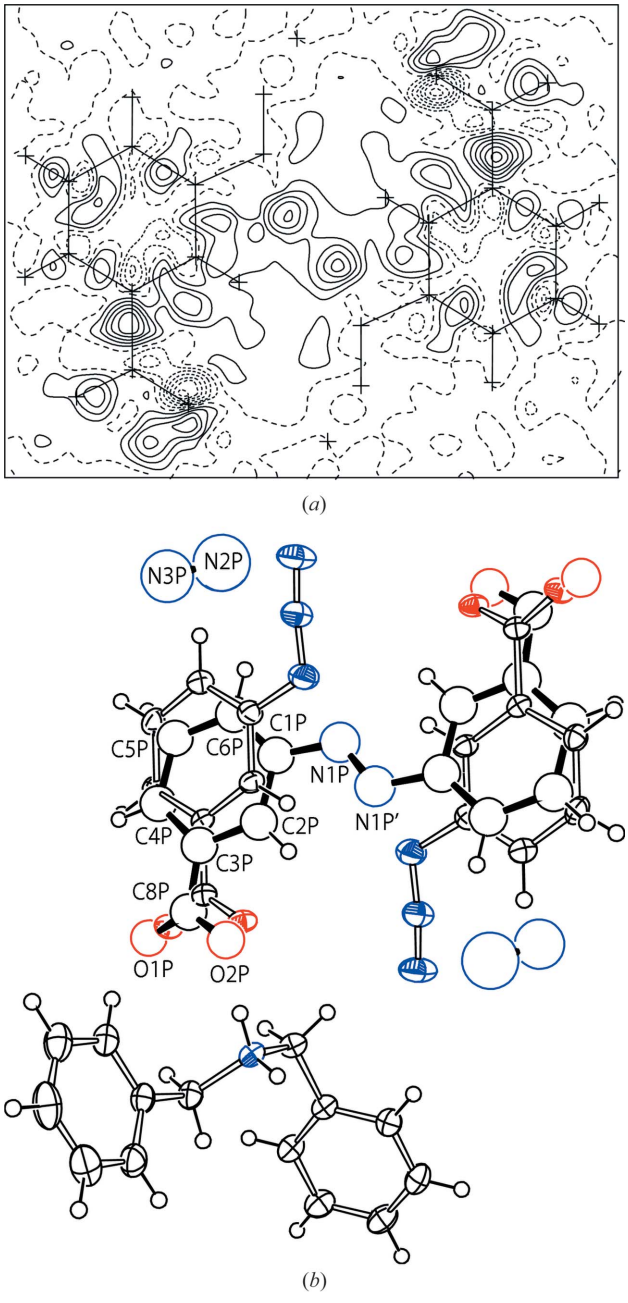

Figure 10
(*a*) Difference electron-density map of (3*a*-db-II) on the average plane of the two 3-azidobenzoic acids around an inversion center; the calculated electron density using atomic positions before photo-irradiation was subtracted from the observed one. Solid and dashed lines indicate the positive and negative electron densities drawn every 0.1 e Å^{-3}. (*b*) Disordered molecular structures after photo-irradiation. The open bonds indicate the original molecules. The molecule with the black bonds is the newly produced 3,3′-dicarboxy-*trans*-azobenzene. The individual isotropic displacement parameters were introduced for the products dinitrogen and *trans*-azobenzene.

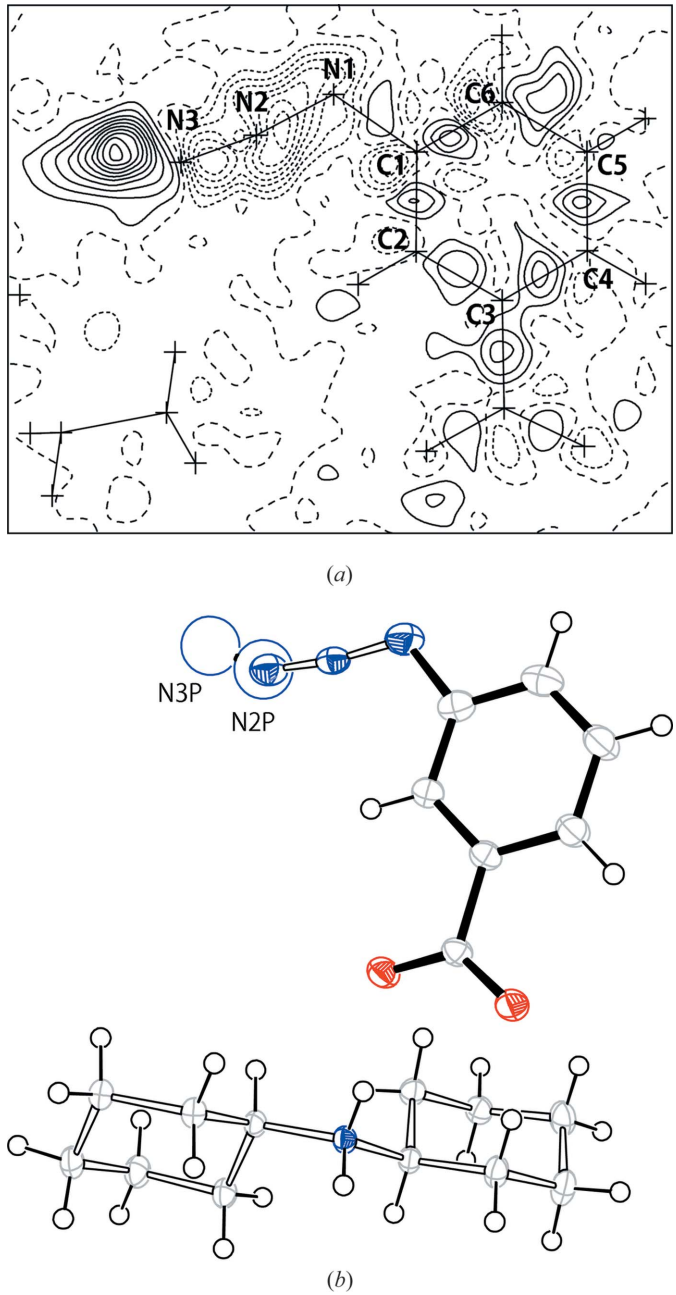

Figure 11
Difference electron-density map of (3*a*-dc) on the plane of the 3-azidobenzoic acid; the calculated electron density using the atomic positions before photo-irradiation was subtracted from the observed one. Solid and dashed lines indicate the positive and negative electron densities drawn every 0.1 e Å^{-3}. (*b*) Disordered molecular structures after photo-irradiation. It was impossible to separate the newly produced 3-carboxynitrene from the original 3-azidobenzoic acid, although the dinitrogen molecule with large isotropic displacement parameters was clearly separated.

The latter factor may be too small, probably owing to the severe overlap with the azido group. The IR spectra showed no peaks due to the formation of azacycloheptatetraene.

4. Discussion

Using acid–base complexes, a variety of reaction pathways for arylnitrenes can be observed. For the (2*a*-db) crystal the intramolecular reaction of the photo-produced nitrene produced a five-membered ring with the neighboring carboxyl group. This is caused by the significantly short distance of the nitreno group and one of the O atoms of the carboxyl group before irradiation, 2.838 (1) Å, compared with the sum of the van der Waals radii of N and O atoms, 3.25 Å. To avoid the steric repulsion with the azido group, the carboxyl group is not coplanar with the phenyl ring before photo-irradiation [dihedral angle 36.8 (2)°]. During photo-irradiation the carboxyl group rotates to have the coplanar conformation with the phenyl ring and easily makes the five-membered ring. On the other hand, the closest intermolecular N1···N1′ contact is 5.630 (1) Å in the crystal before photo-irradiation. Since this distance is too long to make a bond it is impossible to form the dimer molecule, keeping the single-crystal form.

In previous work (Takayama *et al.*, 2003), 1-azido-2-nitrobenzene was transformed to benzofuroxan with the retention of the single-crystal form on exposure to a high-pressure Hg lamp at 80 K for 30 min, as shown in Scheme (II). The intramolecular distance between N1 and one of the O atoms of the nitro group before photo-irradiation is 2.710 (1) Å, which is shorter than the sum of the van der Waals radii (3.07 Å). The dihedral angle between the nitro and phenyl groups is 37.6 (1)° to avoid steric repulsion between the azido and nitro groups. During photo-irradiation the nitro group rotated around the C—N bond of the nitro group and one of the O atoms make a bond with the nitreno group to form a five-membered ring. The reaction process is the same as that of (2*a*-db), although 1,2-dinitrosobenzene was also observed in the IR spectra of 1-azido-2-nitrobenzene.

Dimer molecules were produced for the (3*a*-db-II) and (4*a*-bp) crystals. This is direct evidence that the azobenzene derivatives are produced from arylazides through arylnitrenes, which was first proposed about 85 years ago (Bertho, 1924). The molecular motions in the process of dimerization are different between the two crystals. For (3*a*-db-II) two molecules are situated approximately on the same plane, as shown in Fig. 13(*a*). When the arylnitrenes were produced, they rotated in the opposite direction in the plane and the N═N bond was formed. Since the carboxyl groups are hydrogen bonded to the neighboring dibenzylamine molecules, the molecules should rotate on changing the position of the carboxyl group slightly. The somewhat short distances of the N···O hydrogen bonds after photo-irradiation, 2.66 (3) and 2.45 (3) Å, may be due to the strain of the dimer formation.

On the other hand, two molecules of (4*a*-bp) are not situated on the same plane, as shown in Fig. 13(*b*). Each molecule should rotate around an axis passing through the benzene ring in the opposite direction to each other to be coplanar when the arylnitrene was produced and the N═N bond should be

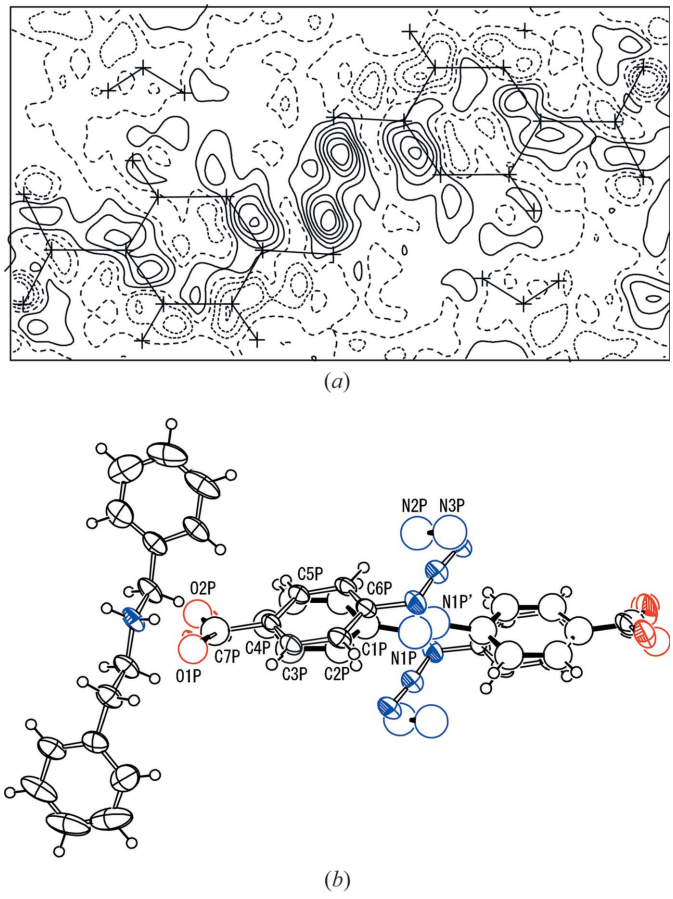

(*a*)

(*b*)

Figure 12
Difference electron-density map of (4*a*-dp) on the average plane composed of the two 4-azidobenzoic acid molecules around an inversion center; the calculated electron density using the atomic positions before photo-irradiation was subtracted from the observed one. Solid and dashed lines indicate the positive and negative electron densities drawn every 0.1 e Å^{-3}. (*b*) Disordered molecular structures after photo-irradiation. The open bonds indicate the original molecules. The molecule with the black bonds is the newly produced 4,4′-dicarboxy-*trans*-azobenzene. The individual isotropic displacement parameters were introduced for the products dinitrogen and *trans*-azobenzene.

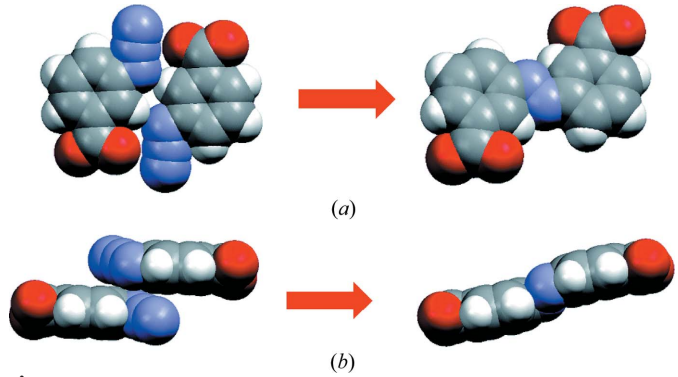

(*a*)

(*b*)

Figure 13
Molecular motion in the process of dimerization for (*a*) (3*a*-db-II) and (*b*) (4*a*-bp). The two nitrenes rotate in the opposite direction in the molecular plane, whereas the two nitrenes rotate in the opposite direction around the axes passing through benzene rings of the respective molecules.

formed. Since the intermolecular hydrogen bonds are formed between the carboxyl group and the neighboring *N*-benzyl-2-phenylethylamine molecule, the carboxyl groups should occupy almost the same positions during photo-irradiation. The intermolecular hydrogen bonds, 2.52 (2) and 2.71 (2) Å after photo-irradiation, are not so different from those before photo-irradiation, 2.669 (1) and 2.691 (2) Å.

For the (3*a*-db-I) and (3*a*-dc) crystals only arylnitrene and dinitrogen appeared after photo-irradiation. The final difference electron-density map of (3*a*-dc) showed a peak beside the C5—C6 bond, as shown in Fig. 11(*a*). The peak position is significantly different from that of the bond electron which appears in the center of the C5—C6 bond. Reproducible data indicating the residual electron density have been obtained. Since the IR spectra suggested the formation of azacycloheptatetraene, the peak height of 0.4 should be assigned to one of the C atoms in azacycloheptatetraene, as shown in Fig. 14. However, the low occupancy factor (< 0.02) and severe overlapping with the original 3-azidobenzoic acid and 3-carboxyphenylnitrene produced make it impossible to separate the whole azacycloheptatetraene molecule from the residual density map. For (3*a*-db-I) there is also a peak beside the C5—C6 bond, as shown in Fig. 9(*a*). This peak also indicates the existence of a seven-membered ring, as indicated in the IR spectra. The IR spectra indicate that a small amount of azacycloheptatetraene is present in the crystal of (3*a*-db-II) after photo-irradiation. However, it was impossible to assign the seven-membered ring in the difference electron-density map, because the peak overlapped with those of the dimer molecule produced.

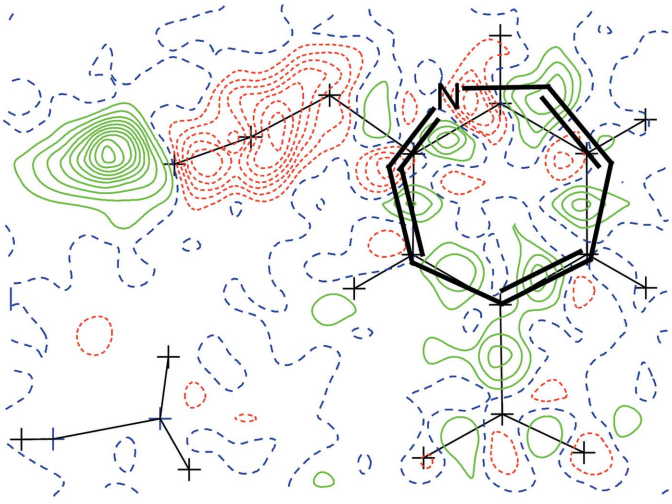

Figure 14
Difference electron-density map of (3*a*-dc) after photo-irradiation, which is the same as that in Fig. 11(*a*). It may be adequate to assume that azacycloheptatetraene with a seven-membered ring was produced in the photo-reaction.

To summarize, the reaction intermediate nitrene and its three different pathways were observed for the arylnitrene, as shown in Fig. 15. If the nitreno group produced is close to the O atom of the neighboring group (less than the sum of the van der Waals contact), a new N—O bond is formed and a new molecule with a five-membered ring is produced. If the nitreno groups of the neighboring molecules are close to each other (less than *ca* 4.5 Å), the two nitreno groups make an N=N bond to form a dimer, the *trans*-azobenzene molecule. The intermolecular hydrogen bonds between the arylnitrene and amine molecules at opposite sides of the N=N bond formation may control the dimer formation with retention of the single-crystal form. If the nitreno group produced is further away from those of the neighboring molecules (greater than *ca* 5.5 Å), the intermediate arylnitrene is kept intact in the crystalline lattice at low temperatures. Moreover, a small portion of azacycloheptatetraene with a seven-membered ring co-exists in the crystalline lattice, which may be produced from the singlet nitrene.

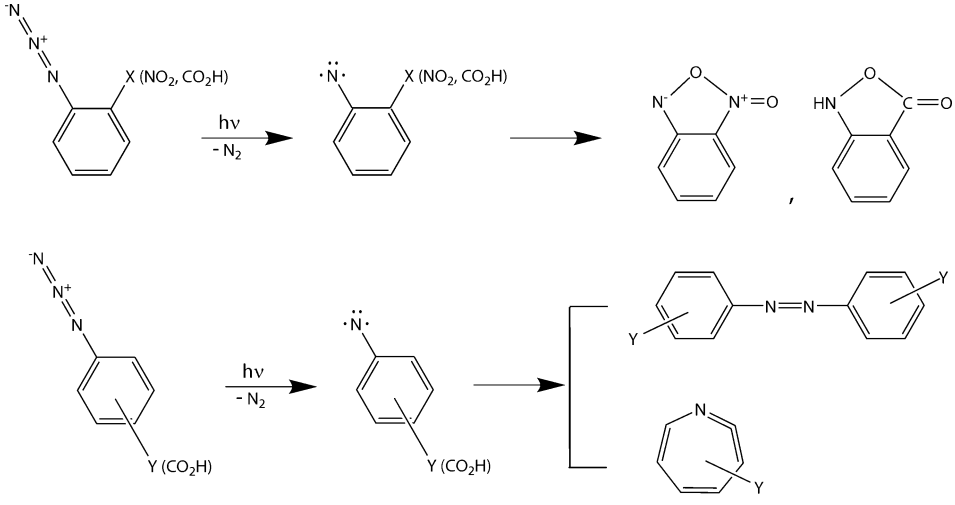

Figure 15
Reaction intermediate nitrene and its three different pathways in the photo-reactions of the arylazides owing to the different crystalline environment. Although the five-membered ring compounds and azobenzene are stable, the seven-membered ring may be easily transformed to the final products if the crystal is warmed to room temperature.

In a previous paper (Takayama *et al.*, 2010) we made a variety of arylazide crystals and irradiated with an Hg lamp to observe the structure of arylnitrene. However, all the crystals except 2-azidobiphenyl decomposed after photo-irradiation. The acid–base complex crystals were made, introducing the carboxyl group to the arylazide molecule as a substituent. The density of the complex crystal becomes significantly smaller than that of the pure arylazide crystal and the reaction cavity of the azido group significantly expanded. The photo reaction can easily occur in the complex crystal whilst retaining the crystallinity. Since the amine molecule shows no light absorption at the wavelengths which cause

nitrene formation, the amine molecule plays the role of reaction matrix in the crystal. In other words, the inactive amine molecule dilutes the reactant molecule in the crystalline state. This will be an indispensable technique in producing an acid–base complex if the reactivity of the molecule is examined in the crystalline state and the unstable intermediates are observed by X-ray analysis.

The authors greatly appreciate Dr Akira Miyazaki of Tokyo Institute of Technology for measuring the ESR spectra. We also thank Professor Tadashi Sugawara and Dr Masaki Kawano of The University of Tokyo for many valuable discussions. This work was partly supported by the Grant-in-Aid for Scientific Research from MEXT.

References

Bertho, A. (1924). *Chem. Ber.* **57**, 1138–1142.
Borden, W. T., Gritsan, N. P., Hadad, C. M., Karney, W. L., Kemnitz, C. R. & Platz, M. S. (2000). *Acc. Chem. Res.* **33**, 765–771.
Born, R., Burda, C., Senn, P. & Wirz, J. (1997). *J. Am. Chem. Soc.* **119**, 5061–5062.
Bruker (2004*a*). *SADABS*. Bruker AXS Inc., Madison, Wisconsin, USA.
Bruker (2004*b*). *XPREP*. Bruker AXS Inc., Madison, Wisconsin, USA.
Bruker (2007). *SAINT*. Bruker AXS Inc., Madison, Wisconsin, USA.
Budruev, A. V., Karyakina, L. N. & Oleinik, A. V. (2003). *High Energy Chem.* **37**, 29–33.
Chapman, O. L. & Roux, J.-P. L. (1978). *J. Am. Chem. Soc.* **100**, 282–285.
Chapman, O. L., Sheridan, R. S. & Roux, J. -P. L. (1978). *J. Am. Chem. Soc.* **100**, 6245–6247.
Crow, W. D. & Wentrup, C. (1967). *Tetrahedron Lett.* **44**, 4379–4384.
Doering, W. E. & Odum, R. A. (1966). *Tetrahedron*, **22**, 81–93.
Dunkin, I. R., Lynch, M. A., AcAlpine, F. & Sweeney, D. (1997). *J. Photochem. Photobiol. Chem.* **102**, 207–212.
Dyall, L. K. & Kemp, J. E. (1967). *Aust. J. Chem.* **20**, 1395–1402.
Farrugia, L. J. (1997). *J. Appl. Cryst.* **30**, 565.
Fomitchev, D. V. & Coppens, P. (1996). *Inorg. Chem.* **35**, 7021–7026.
Fomitchev, D. V., Furlani, T. R. & Coppens, P. (1998). *Inorg. Chem.* **37**, 1519–1526.
Gritsan, N. P. & Plats, M. S. (2001). *Adv. Phys. Org. Chem.* **36**, 255–304.
Gritsan, N. P., Yuzawa, T. & Platz, M. S. (1997). *J. Am. Chem. Soc.* **119**, 5059–5060.
Gritsan, N. P., Zhu, Z., Hadad, C. M. & Platz, M. S. (1999). *J. Am. Chem. Soc.* **121**, 1202–1207.
Hall, J. H., Hill, J. W. & Fargher, J. M. (1968). *J. Am. Chem. Soc.* **90**, 5313–5314.
Harada, J., Uekusa, H. & Ohashi, Y. (1999). *J. Am. Chem. Soc.* **121**, 5809–5810.
Hashizume, D. & Ohashi, Y. (1998). *J. Chem. Soc. Perkin Trans. 2*, pp. 1931–1935.
Hashizume, D. & Ohashi, Y. (1999). *J. Chem. Soc. Perkin Trans. 2*, pp. 1689–1694.
Higashi, T. (1995). *ABSCOR*. Rigaku Corporation, Tokyo, Japan.
Horner, L., Christmann, A. & Gross, A. (1963). *Chem. Ber.* **96**, 399–406.
Hrovat, D. A., Waali, E. E. & Borden, W. T. (1992). *J. Am. Chem. Soc.* **114**, 8698–8699.
Johmoto, K., Sekine, A., Uekusa, H. & Ohashi, Y. (2009). *Bull. Chem. Soc. Jpn*, **82**, 50–57.
Karney, W. L. & Borden, W. T. (2001). *Adv. Carbene Chem.* **3**, 205–251.
Kawano, M., Hirai, K., Tomioka, H. & Ohashi, Y. (2001). *J. Am. Chem. Soc.* **123**, 6904–6908.
Kawano, M., Hirai, K., Tomioka, H. & Ohashi, Y. (2007). *J. Am. Chem. Soc.* **129**, 2383–2391.
Kawano, M., Ishikawa, A., Morioka, Y., Tomizawa, H., Miki, E. & Ohashi, Y. (2000). *J. Chem. Soc. Dalton Trans.* pp. 2425–2431.
Kawano, M., Sano, T., Abe, J. & Ohashi, Y. (1999). *J. Am. Chem. Soc.* **121**, 8106–8107.
Kawano, M., Sano, T., Abe, J. & Ohashi, Y. (2000). *Chem. Lett.* pp. 1372–1373.
Kawano, M., Takayama, T., Uekusa, H., Ohashi, Y., Ozawa, Y., Matsubayashi, K., Imabayashi, H., Mitsimi, M. & Toriumi, K. (2003). *Chem. Lett.* pp. 922–923.
Kim, S.-J., Hamilton, T. P. & Schaefer III, H. F. (1992). *J. Am. Chem. Soc.* **114**, 5349–5355.
Leyva, E. & Platz, M. S. (1985). *Tetrahedron Lett.* **26**, 2147–2150.
Leyva, E., Platz, M. S., Persy, G. & Wirz, J. (1986). *J. Am. Chem. Soc.* **108**, 3783–3790.
Li, Y.-Z, Kirby, J. P., George, M. W., Poliakoff, M. & Schuster, G. B. (1988). *J. Am. Chem. Soc.* **110**, 8092–8098.
Mahé, L., Izuoka, A. & Sugawara, T. (1992). *J. Am. Chem. Soc.* **114**, 7904–7906.
Marcinek, A., Leyva, E., Whitt, D. & Platz, M. S. (1993). *J. Am. Chem. Soc.* **115**, 8609–8612.
Molecular Structure Corporation (1999). *TEXSAN for Windows*. Version 1.06. Molecular Structure Corporation, The Woodlands, Texas, USA.
Naumov, P., Sekine, A., Uekusa, H. & Ohashi, Y. (2002). *J. Am. Chem. Soc.* **124**, 8540–8541.
Ohashi, Y. (1988). *Acc. Chem. Res.* **21**, 268–274.
Ohashi, Y. (1998). *Crystallography Across the Sciences*, edited by H. Schenk, pp. 842–849. Chester: International Union of Crystallography; Copenhagen: Munksgaard.
Ohashi, Y. & Hashizume, D. (1998). *Mol. Cryst. Liq. Cryst.* **313**, 95–104.
Ohashi, Y. & Sasada, Y. (1977). *Nature*, **267**, 142–144.
Ohashi, Y., Yanagi, K., Kurihara, T., Sasada, Y. & Ohgo, Y. (1981). *J. Am. Chem. Soc.* **103**, 5805–5812.
Platz, M. S. (1995). *Acc. Chem. Res.* **28**, 487–492.
Pressprich, M. R., White, M. A., Vekhter, Y. & Coppens, P. (1994). *J. Am. Chem. Soc.* **116**, 5233–5238.
Rigaku (1995). *PROCESS-AUTO*. Rigaku Corporation, Tokyo, Japan.
Rudlinger, M., Schefer, J., Vogt, T., Woike, T., Haussuhl, S. & Zollinger, H. (1992). *Physica B*, **180–181**, 293–298.
Sasaki, A., Izuoka, A. & Sugawara, T. (1996). *Mol. Cryst. Liq. Cryst.* **277**, 17–22.
Sasaki, A., Mahé, L., Izuoka, A. & Sugawara, T. (1998). *Bull. Chem. Soc. Jpn*, **71**, 1259–1275.
Scriven, E. F. V. (1984). *Azides and Nitrenes Reactivity and Utility*. New York: Academic Press.
Sheldrick, G. M. (2008). *Acta Cryst.* A**64**, 112–122.
Siemens (1995). *SMART and SAINT*. Siemens Analytical Instruments, Inc., Madison, Wisconsin, USA.
Smolynsky, G., Wasserman, E. & Yager, W. A. (1962). *J. Am. Chem. Soc.* **84**, 3220–3221.
Takayama, T., Kawano, M., Uekusa, H., Ohashi, Y. & Sugawara, T. (2003). *Helv. Chim. Acta*, **86**, 1352–1358.
Takayama, T., Mitsumori, T., Kawano, M., Sekine, A., Uekusa, H., Ohashi, Y. & Sugawara, T. (2010). *Acta Cryst.* B**66**, 639–646.
Wasserman, E. (1971). *Prog. Phys. Org. Chem.* **8**, 319–337.